

Image Retargetability

Fan Tang, Weiming Dong *Member, IEEE*, Yiping Meng, Chongyang Ma, Fuzhang Wu, Xinrui Li, Tong-Yee Lee, *Member, IEEE*,

Abstract—Real-world applications could benefit from the ability to automatically retarget an image to different aspect ratios and resolutions, while preserving its visually and semantically important content. However, not all images can be equally well processed that way. In this work, we introduce the notion of image retargetability to describe how well a particular image can be handled by content-aware image retargeting. We propose to learn a deep convolutional neural network to rank photo retargetability in which the relative ranking of photo retargetability is directly modeled in the loss function. Our model incorporates joint learning of meaningful photographic attributes and image content information which can help regularize the complicated retargetability rating problem. To train and analyze this model, we have collected a database which contains retargetability scores and meaningful image attributes assigned by six expert raters. Experiments demonstrate that our unified model can generate retargetability rankings that are highly consistent with human labels. To further validate our model, we show applications of image retargetability in retargeting method selection, retargeting method assessment and photo collage generation.

Index Terms—image retargetability, visual attributes, multi-task learning, deep convolutional neural network.

I. INTRODUCTION

CONTENT-AWAR image retargeting (CAIR) addresses the increasing demand to display images on devices of different resolutions and aspect ratios while preserving its visually important content and avoiding noticeable artifacts [1]–[7]. Although state-of-the-art image retargeting techniques can successfully handle more and more images, it is still unclear beforehand whether a specific image can be successfully retargeted. CAIR techniques typically expect the input image containing a mid-size salient object and a relatively simple background, for which most information can be presented within a smaller space. The retargeting results may present severe artifacts if the input images contain rich contents and/or geometric structures that may be damaged. Furthermore, not all the CAIR methods work equally well for the same input. The optimal approach - taking into account quality and robustness - will depend on the input image and the target resolution. For example, warping based retargeting methods [4], [5], [8] are very effective and popular, but will tend to over-stretch or

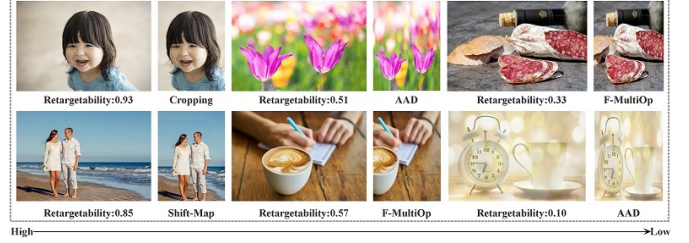


Fig. 1. Retargetability of images predicted by our system. The values are in $[0, 1]$ and a higher value means the image is easy to retarget. For each group, left is the original image, right is the retargeted result generated by the CAIR method suggested by our system.

over-squeeze some contents when salient shapes need to be preserved.

To address the problems of CAIR method selection and result evaluation, in this paper, we introduce the notion of “image retargetability”, i.e., to quantitatively compute how well the image can be retargeted based on its visual content. Fig. 1 shows the predicted retargetability scores of several input images and the corresponding results of the “best” retargeting method selected by our system.

We are inspired by some recent work about quantifying qualitative image properties, such as interestingness [9], memorability [10], synthesizability [11], and mirrorability [12]. To compute image retargetability, we adopt a data-driven methodology and collect a dataset of 13584 sample images from internet photos (Section III). For each image in the dataset, we apply multiple retargeting methods and have six expert raters to label the quality of each retargeting result as one of three levels: good, acceptable, and bad (see Fig. 4 for examples). We also ask the raters to annotate a set of high-level visual attributes for each sample images in the dataset, including repeating patterns, specific geometric structures, perspective, fuzzy, text and shading contrast.

Based on the collected dataset with manual annotations, we propose to measure and analyze image retargetability quantitatively. We demonstrate that there is a strong correlation between image retargetability and other visual attributes. Based on this observation, we leverage deep convolutional neural network and propose a multi-task learning approach by jointly learning visual attributes from deep features and feature sharing for retargetability prediction (Section IV). We evaluate the effectiveness of our framework for image retargetability prediction by comparing against a baseline approach in Section V. Since each CAIR method has its own advantages and limitations, there is no single CAIR algorithm which works better than others in all the cases. We demonstrate how to select the “best” CAIR method using our system. We

F. Tang is with NLPR, Institute of Automation, Chinese Academy of Sciences, Beijing, China and University of Chinese Academy of Sciences, Beijing, China. E-mail: {tangfan2013}@ia.ac.cn.

W. Dong is with Institute of Automation, Chinese Academy of Sciences, Beijing, China. E-mail: {Weiming.Dong}@ia.ac.cn.

Y. Meng is with Didi Chuxing, Beijing, China.

C. Ma is with Snapchat, United States.

F. Wu is with Institute of Software, Chinese Academy of Sciences, Beijing, China.

X. Li is with Department of Mathematics and Physics, North China Electric Power University, Beijing, China.

T. Lee is with National Cheng Kung University, Tainan, Taiwan.

also show that image retargetability is useful for retargeting method assessment and photo collage generation (Section VI).

In summary, our main contributions are:

- We introduce image retargetability as a new quantitative property for image analysis.
- We collect a large image dataset to learn deep features for prediction of image retargetability. The dataset and source code will be released upon final publication.
- We adopt deep neural network and propose a novel multi-task learning architecture to compute the retargetability of a given image.
- We demonstrate that image retargetability can facilitate several applications for image analysis/processing, such as assessment/selection of retargeting method, as well as the generation of photo collages.

II. RELATED WORK

Image retargeting algorithms. The concept of content-aware image retargeting is to preserve important content of an image after resizing operation. Cropping has been widely used to eliminate the unimportant information from the image periphery or improve the overall composition [6], [13], [14], but often destroys the completeness of the objects and causes unexpected loss of information. Discrete methods remove or insert pixels or patches judiciously to preserve content. Seam carving methods iteratively remove a seam in the input image to preserve visually salient content [1], [15]. Shift-map method [3] performs a discrete labeling over individual pixels and retargets an image by removing segments in the net. These approaches are good at retargeting images with rich texture content, but sometimes may cause artifacts of local discontinuity. Continuous methods focus on preserving local structure and usually optimize a warping from the source size to the target size, constrained on its important regions and permissible deformation [8], [16]–[18]. Panozzo et al. [4] minimized warping energy in the space of axis-aligned deformations to avoid unnatural distortions. Kaufmann et al. [19] adopted a finite element method to formulate image warping. Lin et al. [5] presented a patch-based scheme with an extended significance measurement to preserve shapes of both visually salient objects and structural lines. Tan et al. [20] generated feature-preserving constraints in the space of axis-aligned deformations by calculating a feature salience map to guide the warping processing. These approaches can preserve the geometric structure of image content more smoothly but may also permit unwanted less important region to appear in the retargeting result. Multi-operator methods [2], [21], [22] fuse three condensation operators, i.e., seam carving, cropping, and scaling, into a unified optimization framework. Different operators influence each other and are simultaneously optimized to retarget images. Summarization-based methods measure patch similarity and select patch arrangements that well fit together to change the size of an image [23]–[25].

Image retargeting evaluations Rubinstein et al. [26] presented the first comprehensive perceptual study and analysis of image retargeting. They created a benchmark “RetargetMe” and conducted a user study to compare retargeted images

generated by a number of state-of-the-art methods. An overall ranking of the retargeting methods was provided based on user study. Liu et al. [27] proposed an objective quality assessment metric simulating the human vision system to compare image quality by different retargeting methods. Their experiments also suggested that no single method was absolutely superior than others in all the cases. Ma et al. [28] built an image retargeting quality dataset to analyze different retargeting factors including scales, methods, and image content. Zhang et al. [29] analyzed three determining factors for human visual quality of experience, including global structural distortion, local region distortion and loss of salient information. Fang et al. [30] generated a structural similarity map to evaluate if the structural information is well preserved in the retargeted image. Hsu et al. [31] proposed a novel full-reference objective metric for assessing visual quality of a retargeted image based on perceptual geometric distortion and information loss. Bare et al. [32] proposed a new feature and predicted the quality of retargeted images by training a RBF neural network. Zhang et al. [33] adopt a novel aspect ratio similarity metric to measure the geometric change of the images as evidence about how the original image is retargeted. Liang et al. [34] evaluated image retargeting quality through multiple factors including preservation of salient regions, symmetry and global structure, influence of artifacts, and aesthetics. Eye tracking data was also used to improve the performance of objective quality metrics for retargeted images [35]. The above methods evaluate the image retargeting quality through the comparison of original and retargeted images, while in this paper we focus on predicting the quality of retargeting result from the input image itself.

Image property analysis. There has been an increasing interest in analyzing various semantic properties of images. Rosenholtz et al. [36] measured visual clutter of an image which was useful for retrieval of visual content. Kopf et al. [37] analysis the completion of an image and found an optimal crop shape before the completions computed. More recently, unusual photographs were found to be interesting [9], and images of indoor scenes with people were found to be memorable while scenic, outdoor scenes were not [10]. Other qualitative image properties such as popularity [38], colorfulness [39], and aesthetics [40] were also studied. Based on the techniques of example-based texture synthesis, Dai et al. [11] quantified the texture synthesizability as an image property which can be learned and predicted. Moreover, in text-based image retrieval, image specificity [41] with respect to image content and properties was used to discriminate which image was easy to describe.

In this work, we define image retargetability as a semantic property to quantify the probability that an image can be well retargeted. We show that this notion is closely related to deep relative attributes [42].

III. DATASET PREPARATION

In this section, we introduce how we prepare our dataset for investigation of image retargetability. We first collect a large set of images and manually label each image with a few attributes based on the visual content (Section III-A). Then

we apply four typical CAIR methods to all the images in the dataset and manually annotate the quality of each retargeting result (Section III-B).

A. Images and Attributes

Our framework is designed to measure the image retargetability on a wild spectrum of natural images. To this end, it is required that the dataset contains significant variability in terms of contents and compositions. Although the “RetargetMe” benchmark [26] has been widely used in image retargeting works for quality assessment, this dataset only contains 80 images which are not adequate for reliable learning of image attributes. In order to learn retargetability prediction, we prepare an image dataset and manually annotate the sample inputs in terms of retargetability. We have collected 14000 images from Flickr, Pinterest, 500px and Pexels under Creative Commons license by providing 26 keywords acquired from 500px photo categories (see <https://500px.com>). The keywords cover most common categories such as animals, food, nature, sport, travel, still life, fashion and urban exploration. All images are homogeneously scaled by truncating their long sides to 500 pixels, with images smaller than this not being used. We remove some images which are of low quality or heavily watermarked. Finally we add the “RetargetMe” images and have ended up with a dataset of 13584 images.

CAIR methods work best on images where some content can be disposed of. These images typically include either smooth or some regularly-textured areas such as sky, water, or grass. Challenges are posed when the input image contains either rich semantic contents, salient texts, or geometric structures that may be damaged during retargeting. Based on this observation and photography theories [43], we choose a set of attributes that can be mapped to the several major retargeting objectives (preserving content, preserving structure, preserving aesthetics and preventing artifacts), and then manually annotate collected images with these attributes. The selected attributes are: *people and faces*, *lines and/or clear boundaries*, salient *single object*, salient *multiple objects*, *diagonal composition*, *texture*, *repeating patterns*, specific *geometric structures*, *perspective*, *fuzzy*, *text*, *shading contrast*, *content rich* and *symmetry*. Fig. 2 shows some examples in our dataset, along with the attributes assigned to each image. Fig. 3 shows the correlation between image attributes. Besides some attributes with opposite meaning (e.g., a single object vs. multiple objects), most numbers in Fig. 3 have relatively small absolute values which demonstrate that most attributes are uncorrelated to each other.

B. Retargeting Methods and Annotations

To evaluate the retargetability of collected images in the dataset, we have selected and implemented four most typical and commonly used CAIR methods, i.e., multi-operators, inhomogeneous warping, shift-map, and cropping, as described below. We apply these four methods to all the collected images in the dataset.

- *Multi-operators* method outperforms most other approaches according to the comparative study [26]. A typical multi-operators method integrates seam carving,

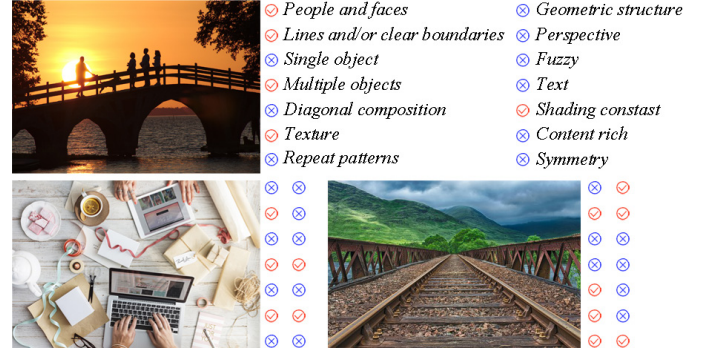


Fig. 2. Example images in our dataset with manually annotated attributes.

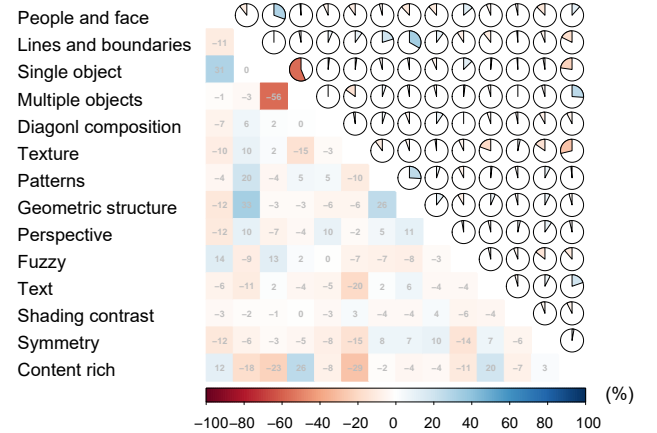


Fig. 3. Correlation among visual attributes.

homogeneous scaling and cropping together to resize an image, and can be considered as a generalized version of seam carving. In our study, we adopt the fast multi-operator method [22] which is fast enough for practical applications.

- *Inhomogeneous warping* based CAIR method is known for its real-time performance and preservation of local continuity. We choose to use the axis-aligned deformation (AAD) method [4], which has been recently verified to be one of the most effective warping methods. Other state-of-the-arts warping-based methods [5], [18], [19] can also be used as the representative method, which will not affect the effectiveness of our retargetability learning and prediction framework.
- *Shift-map* based method can selectively stitch some contents together and usually works well for input with salient contents distributed in different parts of the image. In our study, we apply the original shift-map method [3] to the images in the dataset.
- *Cropping* based CAIR algorithm is preferred in many cases because this kind of methods do not introduce any distortion in the retargeting results [26] and we use the SOAT_{cr} method [6].

Discussions. We have not added summarization-based retargeting methods such as BDS [23] and PM [24] during data collection for two main reasons: first, it usually take

several minutes for this kind of method to generate a good result; second, the results of BDS/PM often present structural mismatch of spatial content [25]. These two artifacts limit its practical use in many applications, especially for some systems which require real-time performance. Moreover, we have not integrated some other CAIR methods which focus on images containing specific contents such as symmetry structure [44], semantically-rich information [7], and textures [25], because our goal is to evaluate image retargetability in a generic way.

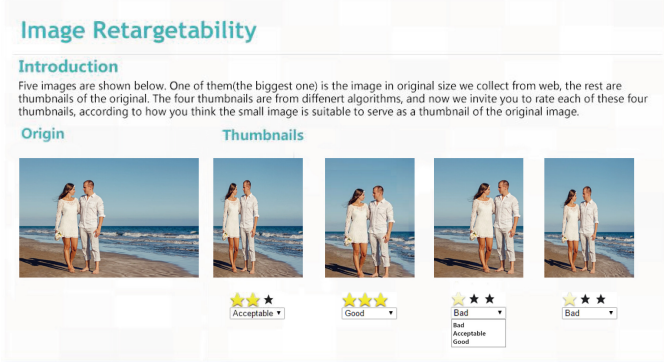


Fig. 4. Our web interface for data annotation.



Fig. 5. An example of importance map used in our framework.

Since most CAIR methods are carefully designed for one-dimensional retargeting, we restrict the change to either the width or the height of the image. For each image in the dataset, we resize its longer dimension to 50% using the four CAIR methods described in Section III-B, all with fixed parameters. Here we choose to retarget to half size as many prior papers about CAIR evaluations do, because most images can be reasonably well handled for smaller size changes while leading to poor results for larger changes. We further guide the CAIR methods by computing a importance map for each image. Specifically, we adopt state of the art saliency detection approaches [45] along with face segmentation [46] and body detector [47] to generate the importance map. Note that the output of a body detector is the bounding box of the body region, we use GrabCut [48] to generate the importance map when a body is detected. We use the average of these maps as our importance map as shown in Fig. 5.

We ask six expert raters to independently evaluate the quality of all the retargeted images and to annotate the result as one of three levels: *good*, *acceptable* and *poor*, which correspond to scores of 1, 0.5 and 0, respectively. Then we compute the average score from the six raters as the evaluation of each retargeting result in the dataset.

Consistency Analysis of Annotations We measure the inter-rater consistency to verify the objectivity of the annotation data. For each image in our dataset, we adopt Kendall's coefficient of

concordance (Kendall's W) [49] to study the rating consistency among different subjects. As a non-parametric statistic measure, Kendall's W ranges from 0 (no consistency) to 1 (completely consistent). The overall average Kendall's W is 0.562 with a standard deviation of 0.0192, raters can get significant concordance on 87.69% images at 0.05 significance level.

IV. MODELING RETARGETABILITY

Based on our dataset, we first analyze the correlation between image attributes and retargetability (Section IV-A). Then we introduce our framework to employ deep learning together with multi-task learning to learn and predict image retargetability (Section IV-B).

A. Measuring Retargetability

For each sample image in the dataset, we define its retargetability as the *max* score of the 4 average user-rated scores (each image has four retargeted outputs and each output image has six user-rated scores, see Section III).

Given this quantitative measurement of retargetability, we can analyze the relationship between different visual attributes and the image retargetability using Rdit analysis [50], which is commonly used in study of ordered categorical data. In Fig. 7, the dashed horizontal line is the reference unit 0.5, and the deviation from reference unit represents the influence of the attribute. Here we can see that some visual attributes are closely related to image retargetability. For example, groups of lines, text, symmetry, geometric and patterns are under the dashed line, which means images with these attributes are more likely to have lower retargetability scores, or equivalently, worse retargeting results annotated by our raters. Images with content rich, diagonal structure and texture often correspond to higher scores. Based on this key observation, we propose to learn and predict retargetability based on visual attributes.

B. Learning and Predicting Retargetability

Although the retargetability of an image is calculated by ratings of retargeted images, retargetability itself is a high-level property of the image. Thus, we aim to learn retargetability directly from source image rather than retargeted images, by utilizing the pre-selected attributes to regularize a pair-wise retargetability ranking training. Fig. 6 shows the overall structure of our model, including a three-level feature representation mechanism as well as two kinds of loss functions corresponding to binary visual features or relative retargetability. We first use the output from deep convolutional network as the low level representation of the image. Then, we learn attribute-specific features for each attribute and finally use this information to learn retargetability. To boost training phase, we learn visual attribute features together with retargetability simultaneously.

In the following, we demonstrate the multi-task learning approach by jointly learning visual attributes from deep features and feature sharing for retargetability.

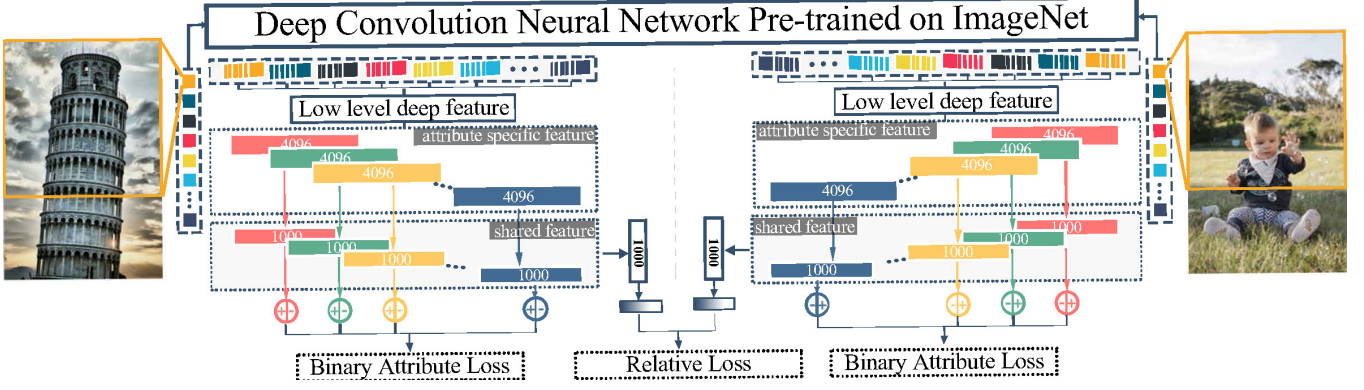


Fig. 6. The overall structure of our method. A siamese network with a three-level feature representation mechanism as well as two kinds of loss function corresponding to binary visual features or relative retargetability is adopted for retargetability learning.

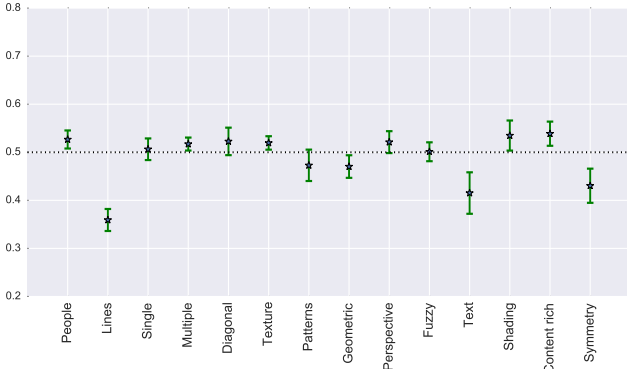


Fig. 7. Ridity scores with 95% confidence interval for visual attributes.

1) *Deep Features*: We use a VGG-19 [51] style model pre-trained on ImageNet [52] for image classification to extract deep representations for input images. The network consists of a stack of convolution layers with pooling and ReLU, followed by three fully-connected layers and finally the softmax with loss. After isotropically re-scaling the input image's short side to 224, we densely crop it to get 224^2 sub-images and feed the square sub-images to the convolutional network as [51]. Note that the need of re-scaling or cropping the image to same size for the learning seems like it would defeat the purpose of studying the effect of change of aspect ratio of an image. However, visual attributes are not damaged by the size change of the input image (i.e., if an image contains a face, the face will still exist even if the aspect ratio of the image has been changed). We denote Fm_i as the last convolutional layer's output of i_{th} sub-image. The low-level deep feature of an input is:

$$Fm = \frac{\sum_{i=1}^K Fm_i}{K},$$

where K is the number of sub-images and is set to 10 in our implementation. We use the output of the convolution layers instead of fully connected layers to get the low-level image representation, so that the output is not too related to the pre-trained classification task.

2) *Learning Retargetability*: Here we try to learn middle-level features for visual attributes and share these features for retargetability to boost learning performance. In our task, visual attributes are all labeled as 1 or -1, such binary

attributes are usually learned by classification method. However, retargetability ranges from 0 to 1, such relative attribute is more powerful in uniquely identifying an image and offers a semantically meaningful way to describe and compare images in the wild [42]. We design different losses for different kind of attributes. Given a low-level deep feature space together with annotated attributes and retargetability-labeled image data, we learn a shared attribute-level feature representation by optimizing a joint loss function that favors both a pair-wise relative loss and a squared hinge loss function with sparsity patterns across binary attributes.

Binary attribute features learning. Given M semantic attributes, the goal is to learn M binary classifiers jointly. Each binary classifier is a four-layer neural network with one input layer, two hidden layers of 4096 and 1000 nodes respectively, and a one-node output layer followed by squared hinge loss function. Inspired by [53], [54], we utilize $l_{2,1}$ -norm minimization to boost feature sharing among different attributes. Multi-task feature learning via $l_{2,1}$ -norm regularization has been studied in many approaches. It encourages multiple predictors from different tasks to share similar parameter sparsity patterns. Given an image i , with a M -dimension label vector L_i element of which is only 1 or -1, supposing parameter of the last hidden layer for the k_{th} attribute servers as w_k , we propose the following equation:

$$loss_{binary}(i) = \sum_{k=1}^M \frac{1}{2} [\max(0, 1 - L_{ik} \cdot L_{ik}^*)]^2 + \frac{1}{2} \alpha \|W\|_{2,1},$$

where $W = [w_k]$ and $\|W\|_{2,1} = \sum \|w_k\|$ is the $l_{2,1}$ -norm of the matrix W .

Relative retargetability learning. In general, the goal of relative attribute learning is to learn ranking functions for labeled image pairs. Existing relative attribute learning approaches learn linear functions to map hand-crafted features to relative scores. Inspired by [55], we collect features learned for each visual attribute as mid-level visual features and use these attribute-related features to train retargetability by a three-layer NN with 1000 hidden nodes. All the shared features are concatenated as the input of the three-layer NN. Instead of using a point-wise regression loss, we adopt a pair-wise loss which has been proved to be more powerful [42], [56]. We define the relative loss as the sum of the contrastive constraint

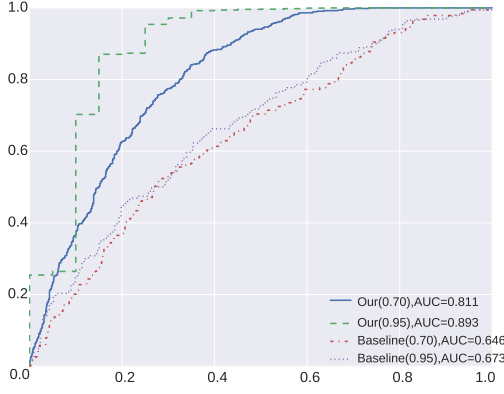


Fig. 8. Comparison of the retargetability prediction accuracy between our method and the baseline approach.

and the similar constraint. Given a pair of images i and j ($i \neq j$), with retargetability y_i and y_j predicted as y_i^* and y_j^* , the loss for the image pair (i, j) is

$$loss_{relative}(i, j) = I(i, j) \cdot l_p(i, j) + (1 - I(i, j)) \cdot l_q(i, j),$$

where

$$I(i, j) = \begin{cases} 1, & y_i > y_j \\ 0, & y_i \sim y_j \end{cases}$$

$$l_p(i, j) = \max(0, \tau - (y_i^* - y_j^*))$$

$$l_q(i, j) = \frac{1}{2}(y_i^* - y_j^*)^2,$$

where $I(i, j)$ is a binary function indicating whether image i and image j have similar retargetability, and $l_p(i, j)$ denotes the contrastive constraint for ordered image pair (i, j) , and $l_q(i, j)$ donates similar constraint for unordered pairs. The parameter τ controls the relative margin among the attribute values when $I(i, j) = 1$.

Formulations and implementations. Given the pair-wise relative loss, we use a two-channel Siamese network as the overall structure [57]. Each channel of the network predicts 16 visual attributes and retargetability together with attribute-specific features. The hinge-based binary loss will be calculated among each group of the M attributes and relative loss is computed by two predicted retargetability. The goal of the entire two-channel network is:

$$\min_{\Theta} J_{\Theta} = \sum_{i,j}^{i \neq j} loss_{binary}(i) + loss_{binary}(j) + loss_{relative}(i, j) + \beta \|\Theta\|_F,$$

where Θ stands for all the parameters to be optimized and $\|\Theta\|_F$ is a regression term to penalize overfitting. We adopt mini-batch stochastic gradient descent with a batch-size of 64 and an initial learning rate of 0.01. During the training stage, we randomly drop out 30% parameters to push the network to learn more general features. During the test stage, we use one way of the siamese network to generate the outputs and truncate the predicted value into $[0, 1]$.

V. EVALUATIONS

This section presents evaluation and analytical results of image retargetability prediction. We randomly select half of

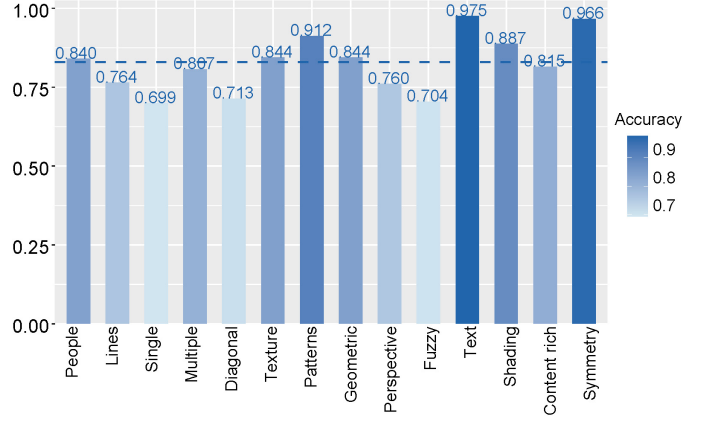


Fig. 9. The accuracy rate for attribute prediction.

the annotated images to train the retargetability predictor and use the rest for testing. This process is performed five times and the average results are reported as below.

Baseline approach. Since our work is the first study of image retargetability, it is difficult to find direct comparisons. Nevertheless, to demonstrate the effectiveness of our framework, we compare our framework with a regression model, which learns retargetability by fine-tuning the VGG-19 network using an euclidean loss as the metric.

Quantitative evaluation. We first use RMSE (root-mean-square error) to evaluate the accuracy of our retargetability prediction approach. The RMSE between our prediction and the ground-truth annotated by the raters is 0.21, while the error for the baseline approach is 0.33. Moreover, since during training our model is more likely to “compare” images with a pair-wise loss rather than learning absolute scores, we need to evaluate how well the predictor can rank all the samples. Specifically, we sort all the testing samples according to their predicted scores and then label each sample as 1 or -1 according to its ground truth retargetability: 1 if the score is larger than a threshold σ , and -1 otherwise. In Fig. 8, we plot the Receiver Operating Characteristic (ROC) curve and report the Area Under Curve (AUC) value by setting σ to 0.95 and 0.7. The results demonstrate that our method is more accurate than the baseline approach, and thus confirms that sharing visual knowledge with high-level image attributes in the predictive model is a compelling way for boosting the learning process. Another reason behind this observation confirms that retargetability is a property dealing with the ability to be resized, any retargetable operations may lead to uncertain results. While in our pipeline, the retargetability is learned on features related to visual attributes which are more insensitive to the input size changing. Furthermore, we report the accuracy for attributes prediction in Fig. 9.

Qualitative evaluation. Figs. 10 and 11 show predicted retargetability and the corresponding retargeted output for several input images. The quality of the retargeted images is well consistent with the predicted retargetability score. As can be seen from the results, images with large homogeneous regions, blurry background and single object lead to higher scores. On the contrary, lower scores are caused by several factors, including salient lines, clear boundaries, geometric

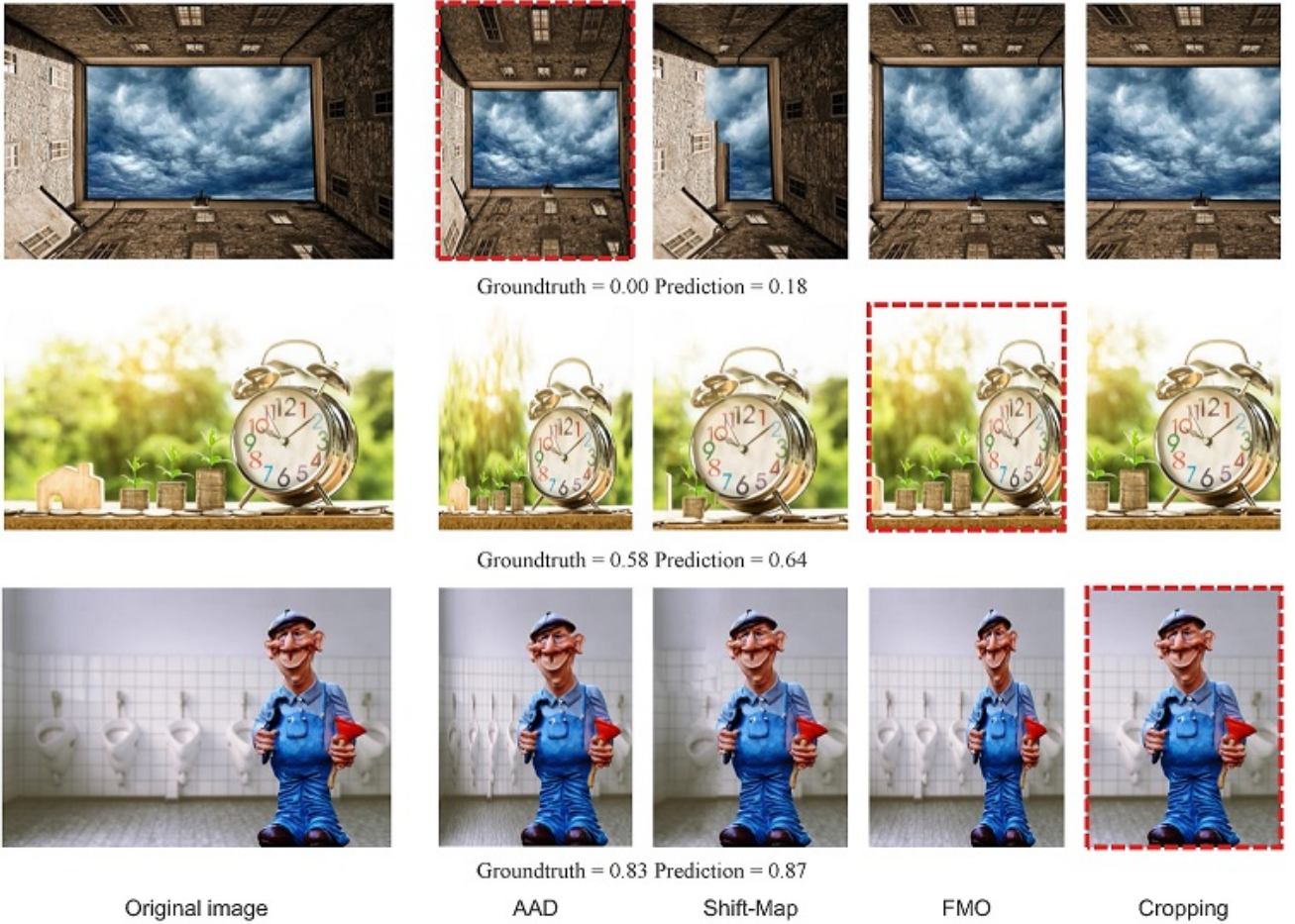


Fig. 10. Examples for retargetability prediction and method selection. In each example, the input image is shown on the left, and the results of the four CAIR methods are shown on the right. The results of the predicted best method are highlighted with red dash lines.

structures, and symmetry.

VI. APPLICATIONS

In this section, we show several applications of image retargetability, including retargeting method selection, retargeting method assessment, and photo collage.

Retargeting method selection. Our system can suggest the “best” retargeting method for a given image. We first collect images which have either “Good” or “Acceptable” retargeting results in our dataset as a new training set, and record the “best” method(s) of each image based on manually annotations (Section III-B). We then fine tune one branch of the trained siamese network by replacing the retargetability prediction layer with a “best” method prediction layer. Note that each image may have more than one “best” method, thus the “best” method prediction layer is in fact a four-node full connected layer followed by sigmoid activation. During training stage, we adopt cross-entropy loss and only fine tune the last two layers of the network. During testing stage, we consider the method which corresponds to the biggest output after activation as the predicted best method for a given input. Fig. 10 shows three such examples, where results of the suggested methods and results of other methods are compared. It can be seen that our “adaptive selection” is superior to random guessing. This is due to the fact the CAIR methods all have their own

philosophies and each one of them works better than others for some images, which necessitates an adaptive selection for the “best” retargeting method for a given image example.

Retargeting method assessment. In this work, we offer a fairly large image dataset together with retargeting annotations which can be used to augment other datasets such as “RetargetMe” [26]. With the help of retargetability, people can easily collect a suitable testing set, which contains a wide range of images with different retargeting difficulties. Apparently, to test if a new CAIR method is effective, it is necessary to use images which are difficult to existing methods. Therefore, since the retargetability of an image can reflect if it can be well retargeted by existing methods, during assessment we can just use more images with low retargetability scores, such as the images in Figs. 11(e) and 11(j). Retargetability can also help people to filter some examples which can be well retargeted by exiting methods, such as the images in Figs. 11(a) and 11(d). In our experiments, we find that the images with retargetability arranging between $(0.0, 0.75]$ are more reliable for new CAIR method assessment.

Photo collage generation. Photo collage is usually created by placing multiple photo images on a canvas of limited size. The input images can be fitted on the canvas by retargeting them at the risk of losing important visual information and making the collage dull. Therefore, optimally selecting image examples

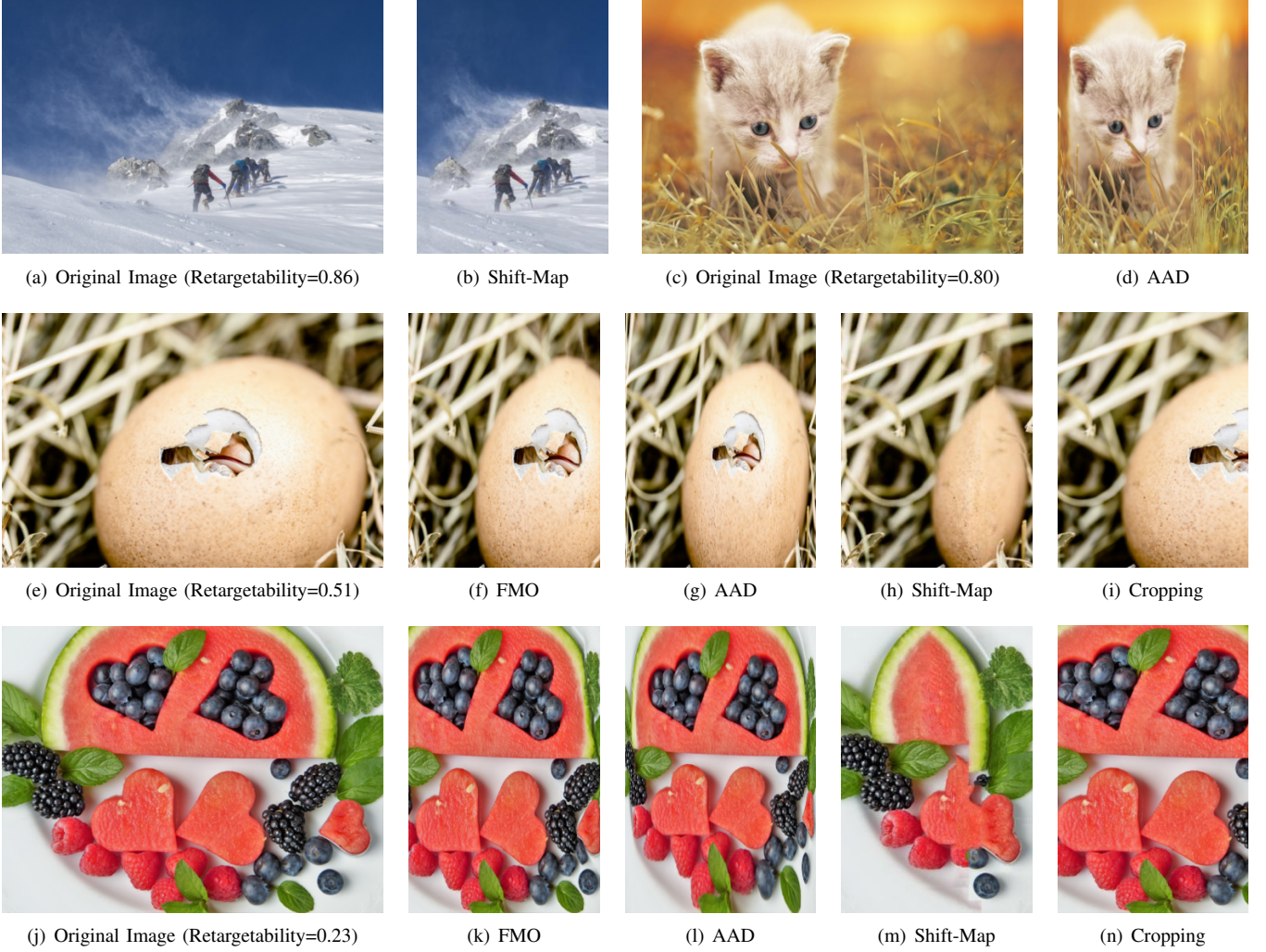


Fig. 11. Images with different retargetability scores and the corresponding results from four select CAIR methods. (e) and (j) are more reliable for assessing new retargeting methods for these images are difficult for existing CAIR methods.

for different sizes of canvas regions is important, since not just any input image can be well retargeted in a given scale. With the notion of image retargetability, automatic graphic design can be more reliable. In Fig. 12 we present an example of using image retargetability to guide the generation of photo collage. The origin photos are shown in Fig. 12(a). Fig. 12(b) shows the result automatically generated by a commercial software¹. All the images in Fig. 12(b) are retargeted by "Best Fit" strategy in the software which sometimes are not reliable. Fig. 12(c) shows the result manually retargeted based on the layout of Fig. 12(b). With the help of retargetability, the collage can be created in a simple but effective way: we first sort all the images based on their retargetability, and then put the images into the canvas in the order of increasing retargetability. Images with relatively lower retargetability are preferentially put into regions where the aspect ratio can be retained to the maximum extent. Fig. 12(d) shows our result of collage generation using this strategy, which preserves more salient content and presents less unnatural cropping artifact compared to Figs. 12(b) and

12(c).

VII. CONCLUSION AND FUTURE WORK

In this paper, we present retargetability as a novel image property and develop a computational predictor for it based on multi-task learning. We construct a large image dataset and annotate the retargetability of each image according to the quality of its retargeted results. We propose a siamese network structure that jointly learns attribute features and the relative retargetability. Our experiments show that image retargetability can be learned and predicted computationally. It can be used to adaptively select a retargeting method for an image, to find feasible image samples for retargeting method evaluation, and to optimize collage layout for graphic design. In our experiments, we only consider the retargetability of an image in one dimension (the long side), which means we restrict the change to either the width or the height of the image. However, retargetability of one image on these two dimensions may not always be the same. As shown in Fig. 13, when we retarget the long side, the resulting images may not be as satisfactory as retargeting the short side. Therefore, in

¹<http://www.collageitfree.com/>



(a) Input photos with various retargetability from low to high



(b) Photo collage result generated by CollageIt (c) Photo collage result generated by CollageIt software and manually retargeted (d) Our photo collage result by using retargetability software

Fig. 12. An example of photo collage generation. We generate photo collage by using retargetability to guide the placement of photos. Our result preserves more salient content and presents less cropping artifact compared to the one from a commercial software.

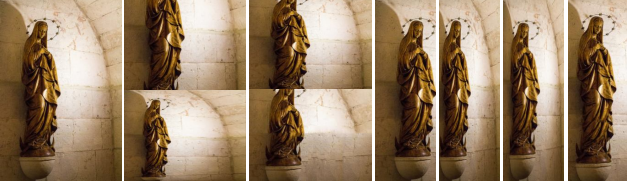


Fig. 13. Retargeting along different dimensions. The input image is shown on the left, the retargeting results along the long dimension and the short one using the four selected CAIR methods are shown in the middle and on the right respectively.

future work we plan to investigate the computation of image retargetability in both dimensions. Another limitation about our method is that we only retarget source images to a fixed scale (50%), but the retargetability of an image varies with the changing of target scale (see examples in supplemental material). We can augment the resulting images and annotate them to analyze the relationship between retargetability and target size in the future. Furthermore, we will try to generalize retargetability for analysis and processing of video data.

REFERENCES

- [1] S. Avidan and A. Shamir, "Seam carving for content-aware image resizing," *ACM Transactions on Graphics*, vol. 26, no. 3, pp. 10:1–10:10, 2007.
- [2] M. Rubinstein, A. Shamir, and S. Avidan, "Multi-operator media retargeting," *ACM Transactions on Graphics*, vol. 28, no. 3, pp. 23:1–23:12, 2009.
- [3] Y. Pritch, E. Kav-Venaki, and S. Peleg, "Shift-map image editing," in *IEEE International Conference on Computer Vision (ICCV)*, 2009, pp. 151–158.
- [4] D. Panozzo, O. Weber, and O. Sorkine, "Robust image retargeting via axis-aligned deformation," *Computer Graphics Forum*, vol. 31, no. 2, pp. 229–236, 2012.
- [5] S.-S. Lin, I.-C. Yeh, C.-H. Lin, and T.-Y. Lee, "Patch-based image warping for content-aware retargeting," *IEEE Transactions on Multimedia*, vol. 15, no. 2, pp. 359–368, 2013.
- [6] J. Sun and H. Ling, "Scale and object aware image thumbnailing," *International Journal of Computer Vision*, vol. 104, no. 2, pp. 135–153, 2013.
- [7] L. Zhang, M. Wang, L. Nie, L. Hong, Y. Rui, and Q. Tian, "Retargeting semantically-rich photos," *IEEE Transactions on Multimedia*, vol. 17, no. 9, pp. 1538–1549, Sept 2015.
- [8] Y.-S. Wang, C.-L. Tai, O. Sorkine, and T.-Y. Lee, "Optimized scale-and-stretch for image resizing," *ACM Transactions on Graphics*, vol. 27, no. 5, pp. 118:1–118:8, 2008.
- [9] M. Gygli, H. Grabner, H. Riemenschneider, F. Nater, and L. V. Gool, "The interestingness of images," in *IEEE International Conference on Computer Vision (ICCV)*. Washington, DC, USA: IEEE Computer Society, 2013, pp. 1633–1640.
- [10] P. Isola, J. Xiao, D. Parikh, A. Torralba, and A. Oliva, "What makes a photograph memorable?" *IEEE Transactions on Pattern Analysis and Machine Intelligence*, vol. 36, no. 7, pp. 1469–1482, July 2014.
- [11] D. Dai, H. Riemenschneider, and L. V. Gool, "The synthesizability of texture examples," in *Proceedings of the 2014 IEEE Conference on Computer Vision and Pattern Recognition*. Washington, DC, USA: IEEE Computer Society, 2014, pp. 3027–3034.
- [12] H. Yang and I. Patras, "Mirror, mirror on the wall, tell me, is the error small?" in *IEEE Conference on Computer Vision and Pattern Recognition (CVPR)*, June 2015, pp. 4685–4693.
- [13] J. Yan, S. Lin, S. B. Kang, and X. Tang, "Learning the change for automatic image cropping," in *IEEE Conference on Computer Vision and Pattern Recognition (CVPR)*, 2013, pp. 971–978.
- [14] L. Zhang, M. Song, Y. Yang, Q. Zhao, C. Zhao, and N. Sebe, "Weakly supervised photo cropping," *IEEE Transactions on Multimedia*, vol. 16, no. 1, pp. 94–107, 2014.
- [15] M. Rubinstein, A. Shamir, and S. Avidan, "Improved seam carving for video retargeting," *ACM Transactions on Graphics*, vol. 27, no. 3, pp. 16:1–16:10, 2008.
- [16] L. Wolf, M. Guttman, and D. Cohen-Or, "Non-homogeneous content-driven video-retargeting," in *International Conference on Computer Vision (ICCV)*, Oct 2007, pp. 1–6.
- [17] Y. F. Zhang, S. M. Hu, and R. R. Martin, "Shrinkability maps for content-aware video resizing," *Computer Graphics Forum*, vol. 27, no. 7, pp. 1797–1804, 2008.

- [18] P. Krähenbühl, M. Lang, A. Hornung, and M. Gross, "A system for retargeting of streaming video," *ACM Trans. Graph.*, vol. 28, no. 5, pp. 126:1–126:10, 2009.
- [19] P. Kaufmann, O. Wang, A. Sorkine-Hornung, O. Sorkine-Hornung, A. Smolic, and M. Gross, "Finite element image warping," *Computer Graphics Forum*, vol. 32, no. 2pt1, pp. 31–39, 2013.
- [20] W. Tan, B. Yan, K. Li, and Q. Tian, "Image retargeting for preserving robust local feature: Application to mobile visual search," *IEEE Transactions on Multimedia*, vol. 18, no. 1, pp. 128–137, Jan 2016.
- [21] W. Dong, N. Zhou, J.-C. Paul, and X. Zhang, "Optimized image resizing using seam carving and scaling," *ACM Transactions on Graphics*, vol. 28, no. 5, pp. 125:1–125:10, 2009.
- [22] W. Dong, G. Bao, X. Zhang, and J.-C. Paul, "Fast multi-operator image resizing and evaluation," *Journal of Computer Science and Technology*, vol. 27, no. 1, pp. 121–134, 2012.
- [23] D. Simakov, Y. Caspi, E. Shechtman, and M. Irani, "Summarizing visual data using bidirectional similarity," in *IEEE Conference on Computer Vision and Pattern Recognition (CVPR)*, June 2008, pp. 1–8.
- [24] C. Barnes, E. Shechtman, A. Finkelstein, and D. B. Goldman, "Patch-match: a randomized correspondence algorithm for structural image editing," *ACM Transactions on Graphics*, vol. 28, no. 3, pp. 24:1–24:12, 2009.
- [25] W. Dong, F. Wu, Y. Kong, X. Mei, T.-Y. Lee, and X. Zhang, "Image retargeting by texture-aware synthesis," *IEEE Transactions on Visualization and Computer Graphics*, vol. 22, no. 2, pp. 1088–1101, 2016.
- [26] M. Rubinstein, D. Gutierrez, O. Sorkine, and A. Shamir, "A comparative study of image retargeting," *ACM Transactions on Graphics*, vol. 29, no. 6, pp. 160:1–160:10, 2010.
- [27] Y.-J. Liu, X. Luo, Y.-M. Xuan, W.-F. Chen, and X.-L. Fu, "Image retargeting quality assessment," in *Computer Graphics Forum*, vol. 30, no. 2. Wiley Online Library, 2011, pp. 583–592.
- [28] L. Ma, W. Lin, C. Deng, and K. N. Ngan, "Image retargeting quality assessment: A study of subjective scores and objective metrics," *IEEE Journal of Selected Topics in Signal Processing*, vol. 6, no. 6, pp. 626–639, Oct 2012.
- [29] J. Zhang and C.-C. J. Kuo, "An objective quality of experience (QoE) assessment index for retargeted images," in *Proceedings of the ACM International Conference on Multimedia*, ser. MM '14. New York, NY, USA: ACM, 2014, pp. 257–266.
- [30] Y. Fang, K. Zeng, Z. Wang, W. Lin, Z. Fang, and C. W. Lin, "Objective quality assessment for image retargeting based on structural similarity," *IEEE Journal on Emerging and Selected Topics in Circuits and Systems*, vol. 4, no. 1, pp. 95–105, March 2014.
- [31] C.-C. Hsu, C.-W. Lin, Y. Fang, and W. Lin, "Objective quality assessment for image retargeting based on perceptual geometric distortion and information loss," *IEEE Journal of Selected Topics in Signal Processing*, vol. 8, no. 3, pp. 377–389, 2014.
- [32] B. Bare, K. Li, W. Wang, and B. Yan, "Learning to assess image retargeting," in *ACM International Conference on Multimedia*, 2014, pp. 925–928.
- [33] Y. Zhang, Y. Fang, W. Lin, X. Zhang, and L. Li, "Backward registration based aspect ratio similarity (ars) for image retargeting quality assessment," *IEEE Transactions on Image Processing*, vol. 25, no. 9, pp. 4286–4297, 2016.
- [34] Y. Liang, Y.-J. Liu, and D. Gutierrez, "Objective quality prediction of image retargeting algorithms," *IEEE Transactions on Visualization and Computer Graphics*, vol. 23, no. 2, pp. 1099–1110, Feb 2017.
- [35] S. Castillo, T. Judd, and D. Gutierrez, "Using eye-tracking to assess different image retargeting methods," in *Proceedings of the ACM SIGGRAPH Symposium on Applied Perception in Graphics and Visualization*. New York, NY, USA: ACM, 2011, pp. 7–14.
- [36] R. Rosenholtz, Y. Li, and L. Nakano, "Measuring visual clutter," *Journal of Vision*, vol. 7, no. 2, pp. 17:1–17:22, 2007.
- [37] J. Kopf, W. Kienzle, S. Drucker, and S. B. Kang, "Quality prediction for image completion," *Acm Transactions on Graphics*, vol. 31, no. 6, p. 131, 2012.
- [38] A. Khosla, A. Das Sarma, and R. Hamid, "What makes an image popular?" in *Proceedings of the 23rd international conference on World wide web*. ACM, 2014, pp. 867–876.
- [39] C. Amati, N. J. Mitra, and T. Weyrich, "A study of image colourfulness," in *Proceedings of the Workshop on Computational Aesthetics*, ser. CAe '14. New York, NY, USA: ACM, 2014, pp. 23–31.
- [40] X. Lu, Z. Lin, H. Jin, J. Yang, and J. Z. Wang, "Rating image aesthetics using deep learning," *IEEE Transactions on Multimedia*, vol. 17, no. 11, pp. 2021–2034, Nov 2015.
- [41] M. Jas and D. Parikh, "Image specificity," in *IEEE Conference on Computer Vision and Pattern Recognition (CVPR)*, June 2015, pp. 2727–2736.
- [42] X. Yang, T. Zhang, C. Xu, S. Yan, M. S. Hossain, and A. Ghoneim, "Deep relative attributes," *IEEE Transactions on Multimedia*, vol. 18, no. 9, pp. 1832–1842, Sept 2016.
- [43] L. Yao, P. Suryanarayan, M. Qiao, J. Z. Wang, and J. Li, "Oscar: On-site composition and aesthetics feedback through exemplars for photographers," *International Journal of Computer Vision*, vol. 96, no. 3, pp. 353–383, 2012.
- [44] H. Wu, Y.-S. Wang, K.-C. Feng, T.-T. Wong, T.-Y. Lee, and P.-A. Heng, "Resizing by symmetry-summarization," *ACM Transactions on Graphics*, vol. 29, no. 6, pp. 159:1–159:10, 2010.
- [45] M. M. Cheng, N. J. Mitra, X. Huang, P. H. S. Torr, and S. M. Hu, "Global contrast based salient region detection," *IEEE Transactions on Pattern Analysis and Machine Intelligence*, vol. 37, no. 3, pp. 569–582, 2015.
- [46] S. Saito, T. Li, and H. Li, "Real-time facial segmentation and performance capture from rgb input," 2016.
- [47] S. Ren, K. He, R. Girshick, and J. Sun, "Faster r-cnn: Towards real-time object detection with region proposal networks," *IEEE Transactions on Pattern Analysis and Machine Intelligence*, vol. PP, no. 99, pp. 1–1, 2015.
- [48] C. Rother, V. Kolmogorov, and A. Blake, "Grabcut: Interactive foreground extraction using iterated graph cuts," in *ACM transactions on graphics (TOG)*, vol. 23, no. 3. ACM, 2004, pp. 309–314.
- [49] M. G. Kendall and B. B. Smith, "The problem of m rankings," *The Annals of Mathematical Statistics*, vol. 10, no. 3, pp. 275–287, 09 1939.
- [50] J. L. Devore, *Probability and Statistics for Engineering and the Sciences*. Cengage Learning, 2015.
- [51] K. Simonyan and A. Zisserman, "Very deep convolutional networks for large-scale image recognition," *Computer Science*, 2014.
- [52] O. Russakovsky, J. Deng, H. Su, J. Krause, S. Satheesh, S. Ma, Z. Huang, A. Karpathy, A. Khosla, M. Bernstein, A. C. Berg, and L. Fei-Fei, "ImageNet Large Scale Visual Recognition Challenge," *International Journal of Computer Vision*, vol. 115, no. 3, pp. 211–252, 2015.
- [53] J. Liu, S. Ji, and J. Ye, "Multi-task feature learning via efficient $l_{2,1}$ -norm minimization," in *Proceedings of the Twenty-Fifth Conference on Uncertainty in Artificial Intelligence*. Arlington, Virginia, United States: AUAI Press, 2009, pp. 339–348.
- [54] A. H. Abdunabi, G. Wang, J. Lu, and K. Jia, "Multi-task cnn model for attribute prediction," *IEEE Transactions on Multimedia*, vol. 17, no. 11, pp. 1949–1959, Nov 2015.
- [55] S. J. Hwang, F. Sha, and K. Grauman, "Sharing features between objects and their attributes," in *IEEE Conference on Computer Vision and Pattern Recognition (CVPR)*, June 2011, pp. 1761–1768.
- [56] D. Parikh and K. Grauman, "Relative attributes," in *IEEE International Conference on Computer Vision*, Nov 2011, pp. 503–510.
- [57] S. Zagoruyko and N. Komodakis, "Learning to compare image patches via convolutional neural networks," in *Proceedings of the IEEE Conference on Computer Vision and Pattern Recognition*, 2015, pp. 4353–4361.



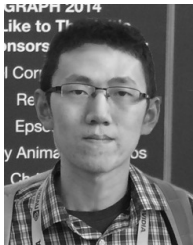
Fan Tang received the BSc degree in computer science from North China Electric Power University in 2013. He is currently working toward the PhD degree in National Laboratory of Pattern Recognition, Institute of Automation, Chinese Academy of Sciences. His research interests include computer graphics, computer vision and machine learning.



Weiming Dong is a Professor in the Sino-European Lab in Computer Science, Automation and Applied Mathematics (LIAMA) and National Laboratory of Pattern Recognition (NLPR) at Institute of Automation, Chinese Academy of Sciences. He received his BSc and MSc degrees in Computer Science in 2001 and 2004, both from Tsinghua University, China. He received his PhD in Computer Science from the University of Lorraine, France, in 2007. His research interests include image synthesis and image recognition. Weiming Dong is a member of the ACM



Yiping Meng received the BSc degree in Software Engineering from University of Electronic Science and Technology of China in 2013. In 2017, she received the MEng degree in National Laboratory of Pattern Recognition, Institute of Automation, Chinese of Sciences. Her research interests include computer vision, image processing, and information visualization.



Chongyang Ma received the B.S. degree from the Fundamental Science Class (Mathematics and Physics) of Tsinghua University in 2007 and the Ph.D. degree in computer science from the Institute for Advanced Study of Tsinghua University in 2012. He spent one year as a Post-Doctoral Fellow with the Department of Computer Science, University of British Columbia. He is currently a Post-Doctoral Scholar with the Department of Computer Science, University of Southern California.



Fuzhang Wu received the PhD candidate in the Sino-European Lab in Computer Science, Automation and Applied Mathematics (LIAMA) and National Laboratory of Pattern Recognition (NLPR) at Institute of Automation, Chinese Academy of Sciences (CASIA). He received his BSc in computer science in 2010 from Northeast Normal University, P. R. China. His research interests include image synthesis and image analysis. He is currently a Post-Doctoral Scholar with Institute of Software, Chinese Academy of Sciences.



Xinrui Li received the BEc degree in statistics from Shandong University of Finance and Economics in 2016. She is currently pursuing the master degree in the Department of Mathematics, North China Electric Power University. Her research interests include applied statistics, Mathematical Statistics, and machine learning.



Tong-ye Lee received the PhD degree in computer engineering from Washington State University, Pullman, in May 1995. He is currently a chair professor in the Department of Computer Science and Information Engineering, National Cheng-Kung University, Tainan, Taiwan, ROC. He leads the Computer Graphics Group, Visual System Laboratory, National Cheng-Kung University (<http://graphics.csie.ncku.edu.tw/>). His current research interests include computer graphics, non-photorealistic rendering, medical visualization, virtual

reality, and media resizing. He is a senior member of the IEEE and the member of the ACM.